

Laser remote sensing in atmosphere investigation

D. NICOLAE*, L. BELEGANTE, A. NEMUC

National Institute of Research and Development for Optoelectronics, 409 Atomistilor Street, RO-077125
Măgurele, Ilfov, Romania

One of the main issues at the Romanian Atmospheric 3D research Observatory - RADO refers to direct and indirect effect of aerosols on radiative budget. Vertically resolved profiles of optical properties of aerosols and ozone are measured each day by lidars. First information which can be immediately extracted is the vertical structure of the atmosphere. In this study, the multi-wavelength Raman lidar is used to observe significant variations in aerosol characteristics depending on the particle origins. The height of layers in the lower troposphere is calculated using the gradient method - minima of the first derivative – of the range corrected lidar signal. Optical properties of aerosols are derived in order to assess the aerosol class, which is then confirmed or not by air mass backward trajectory analysis.

(Received November 22, 2010; accepted November 29, 2010)

Keywords: LIDAR, Atmosphere, Long-range transport

1. Introduction

Both air quality process studies and climate impact investigations require information about the vertical distribution of aerosols in the atmosphere as well as about their interactions with other atmospheric components (gaseous precursors, water vapor, ozone). Aerosol chemical and physical properties have been found (IPCC, 2007) to have a strong direct and indirect impact on earth's radiative budget. Aerosols scatter and absorb both incoming solar radiation and outgoing terrestrial radiation. The amount of radiation that is scattered and the directions of scatter, as well as the amount of radiation is absorbed, varies with aerosol composition, size, and shape. Thus, the physical properties of aerosols determine whether they contribute to the net heating or cooling of the Earth's climate. The indirect effect of aerosols originates from modification of cloud microphysical and optical properties and of the earth's hydrological cycle.

To quantify the impact of aerosols on climate and to assess, in turn, the feedback of climate change on aerosols requires a thorough understanding of the physico-chemical aerosol processes on the micro-scale and aerosol evolution in the context of regional and global scale circulation.

The high variability of physical and optical properties of particles linked to meteorological parameters such as temperature, humidity and wind speed require studies of the aerosols in their natural state. Over the past several years, aerosol features have been intensively investigated through numerical modeling [1, 2] and thanks to experiments [1-3] detailed information on aerosol physical and optical properties can be provided by *ground-based in situ measurements*. Unfortunately these observations often remain limited to the ground. However, ground level concentrations can also be influenced by vertical transport induced by turbulent mass flux. Even more importantly, the direct and indirect climate impact of aerosols depends on the total aerosol load in the atmospheric column and its vertical distribution. Dubovik et al. [4] ascertain aerosol

features in extensively measuring *solar transmission and sky radiation*, but results of such passive measurements are averaged over the entire atmospheric column and cannot provide information regarding the vertical distribution of particles.

Laser remote sensing (lidar) technology turned out to be an appropriate tool in the determination of particle optical properties [5] [6], and ozone concentrations [7] either from ground, airplanes or space.

2. Methodology

2.1 Principle of lidar detection

LIDARs (LIght Detection And Ranging) are laser based systems for atmosphere sounding, which allow suspended particulate detection along the sounding direction, with a very good precision and in a very short time (seconds).

Probing the atmosphere with a laser is similar to using radar, with the difference that the lidar uses electromagnetic radiation (light) from the optical domain instead of radio waves. The LIDAR technique is an active method because it uses an artificial light source for the retrieval of atmospheric parameters. This contrasts with passive methods, which use light emission from natural light sources (sun, moon) or thermal emission.

Lidars make use of a laser to excite backscattering in the atmosphere. This backscattered signal is observed using a telescope receiver, which collects the light and send it to the receiver optics. The role of the optical chain is to select specific wavelengths, split between them and direct them to photodetectors, which convert the optical signal into electrical signals. Not only that vertical distribution of aerosols, ozone and wind can be measured, but their temporal dynamics can be assessed by long-term monitoring, since the response of the instrument is real time.

A typical LIDAR system (Fig. 1) consists of a transmitter and a receiver.

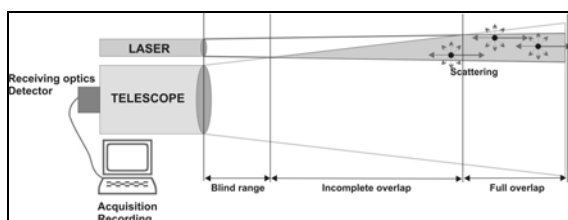


Fig. 1. Basic principle of lidar systems.

The transmitter emits short-time laser pulses into the atmosphere. The laser emission is *specific* - it has a small spatial divergence light beam, and it is quasi-monochromatic and coherent -- and it can emit very high power density, short time pulses (e.g. 100 mJ at 532 nm, pulse width ~ 3 ns, laser repetition rate at 50 Hz). The laser beam interacts with the atmospheric constituents as it propagates through a multitude of phenomena such as elastic light scattering (molecular-Rayleigh, aerosols-Mie), and inelastic (molecular - Raman) light scattering, fluorescence and absorption. A receiving telescope collects a very small fraction of the backscattered light. In addition to the telescope, the receiver usually contains a polychromatic filter for the spectral separation, high sensitivity photodetectors, and fast sampling rate analog-to-digital converters. The magnitude of the received signal is proportional to the number density of the atmospheric diffusers (molecules or aerosols), their intrinsic properties (i.e. probability of interaction with the electromagnetic radiation at the laser wavelengths, called cross-section value) and with the laser incident energy.

Although there are general aspects that apply to all systems, the design of a lidar is always dependent on the application. For example, the type of laser used in a lidar system depends on the physical quantity that the lidar has been designed to measure. Some measurements require a very specific wavelength (i.e., resonance-fluorescence) or wavelengths (i.e., DIAL) and can require complex laser systems to produce these wavelengths, whereas other lidars can operate across a wide wavelength range (i.e., Rayleigh, Raman and aerosol lidars). The power and pulse-repetition frequency of a laser must also match the requirements of the measurements.

Although lidars have many advantages comparing with ground-level instruments for atmospheric monitoring and even with passive remote sensing (ground-based, such as microwave radiometry or sun photometry, or satellite-based), there are limitations due to current technological and mathematical developments.

Main drawbacks of ground-based lidars are local operation (and therefore relevance) coupled with a sparse territorial distribution and the limited information that can be derived directly. Beyond the difficulties in calibrating a lidar system (either Mie, Raman or water vapor channels), complementary information is required in order to quantitatively derive optical parameters or concentration.

This is due to the non-determination in the lidar equation. The solution of this equation can be obtained only by assuming a certain relation between backscatter and extinction coefficient, e.g. by assessing the lidar ratio for the entire lidar profile in case of elastic detection.

During the past decade sophisticated computational procedures have been developed and successfully tested and can be used for the retrieval of microphysical properties of particles such as volume and surface-area concentration, effective radius, refractive index characteristics, and single-scattering albedo from optical data provided by lidars [8-10]. A minimum number of three measurement wavelengths [11] as well as a combination of particle backscatter and particle extinction coefficients [8], [11] are needed for a successful retrieval of microphysical particle properties. The needed optical data are measured with multi-wavelength Raman lidars.

The retrieval of the physical and chemical aerosol properties from the optical measurements is a highly non-trivial and challenging task. It is often not possible to extract the full information about the aerosol field from observations at fixed sites and for a limited set of wavelength channels. Even using multiwavelength lidar data microphysical parameters can only be roughly assessed. This is due to the limitation of accuracy and range. Moreover, without a detailed assessment of system's capability and status (alignment, noise perturbation, response linearity etc.), is impossible to identify and correct possible artefacts in the signal, which can corrupt drastically the final parameters.

2.2 The multiwavelength Raman lidar

Since the end of 2005, monitoring of long range transported aerosols is regularly performed at Magurele site (44.35 N, 26.03E), in the SSW part of Bucharest, using a multiwavelength lidar system RALI. The laser radiation of RALI is emitted at 1064, 532 and 355nm and collected at 1064, 532p (parallel), 532s (cross), 355, 607, 387 and 408 nm. In order to increase the dynamic range, almost all channels have both analog and photon counting detection (analog for the lower troposphere and photon counting for the upper troposphere).

2.3 Aerosol optical parameters

To analyze the return signal in laser remote sensing means to find solutions for the equation which relates the characteristics of the received and emitted signal, and the propagation medium. The form of the equation depends of the interaction type. In this study, we used a simplified form of the lidar equation that is appropriate for monostatic lidar, i.e. with parallel transmitter and receiver axes, without any high-spectral resolution components. This equation is applicable to simple Rayleigh, vibrational Raman, and DIAL systems. It is not appropriate for Doppler or pure rotational Raman lidar, because it does not include the required spectral dependencies.

The magnitude of the received lidar signal is proportional to the number density of the atmospheric

diffusers (molecules or aerosols), their intrinsic properties (i.e. probability of interaction with the electromagnetic radiation at the laser wavelengths, called cross-section value) and with the laser incident energy. The number of photons incident on the collecting optic of the lidar due to scattering of type i is

$$N_r^i = P \tau_i(\lambda_L) A \int_{R_1}^{R_2} \frac{1}{r^2} T_{\rightarrow}(r, \lambda_L) T_{\leftarrow}(r, \lambda_D) \xi(r) \sigma_{\pi}^i(\lambda_L) N^i(r) dr \quad (1)$$

where P as the total number of photons emitted by the laser in a single laser pulse at the laser wavelength λ_L , τ as the transmission coefficient of the lidar transmitter optics, A is the area of the collecting optics, $T_{\rightarrow}(r, \lambda_L)$ is the optical transmission of the atmosphere at the laser wavelength, along the laser path to the range r , λ_D is the wavelength of the detected (scattered) light, $\sigma_{\pi}^i(\lambda_L)$ is the backscatter cross section for scattering of type i at the laser wavelength, and $\xi(r)$ is the overlap factor that takes into account the intensity distribution across the laser beam and the physical overlap of the transmitted laser beam on the FOV of the receiver optics. The term $1/r^2$ in Eq. 1 arises from the decreasing illuminance incident on the telescope surface by the scattered light, as the range increases.

The forward and backward transmission of the atmosphere can be expressed as:

$$T_{\rightarrow}(\lambda_L, R) = \exp\left[-\int_{R_1}^{R_2} \alpha(\lambda_L, r) dr\right] \quad (2)$$

$$T_{\leftarrow}(\lambda_D, R) = \exp\left[-\int_{R_2}^{R_1} \alpha(\lambda_D, r) dr\right] \quad (3)$$

The atmospheric backscattering coefficient $\beta(\lambda, R)$, is a key element of the lidar equation Eq. 1-26 and is proportional to the cross section of the involved physical process $\sigma(\lambda_L, \lambda_D, R)$ and to the number density $N(R)$ of the atmospheric active diffusers (i.e. atoms, molecules, particles, clouds) in the probed volume. The parameters $\alpha(\lambda, R)$, $\beta(\lambda, R)$ and $\sigma(\lambda_L, \lambda_D, R)$ refers to all possible physical interactions within the atmosphere.

When the lidar equation is adapted to the specific process involved (i.e. Rayleigh, Mie, Raman), various atmospheric properties and parameters can be retrieved. An ideal lidar that can explore all these processes is obviously a multiwavelength system. The β [$\text{m}^{-1}\text{sr}^{-1}$] and α [m^{-1}] coefficients may be expressed as the sum of the aerosols (a), molecular (m) and trace gases (t) contributions:

$$\begin{aligned} \beta(\lambda_L, R) &= \beta_a(\lambda_L, R) + \beta_m(\lambda_L, R) + \beta_t(\lambda_L, R) \\ \alpha(\lambda_L, R) &= \alpha_a(\lambda_L, R) + \alpha_m(\lambda_L, R) + \alpha_t(\lambda_L, R) \end{aligned} \quad (4)$$

The effect of tracegases will be neglected due to the very weak contribution of backscatter and absorption of trace gases at wavelengths used for elastic lidar.

Multiple scattering is also neglected in Eq. 1-32 although this assumption has clear limitations.

As described in [12], the backscatter and extinction coefficients can be retrieved from elastic backscatter and inelastic Raman detection, respectively. Therefore, using both techniques, it could be possible to extract both parameters simultaneously. Advanced lidar systems with elastic and inelastic channels deliver in the same time elastic and inelastic Raman signals, which can be fed into the inversion to obtain all optical parameters, because they describe the same atmosphere.

Usually, Nitrogen molecules are used to obtain the Raman signal, due to the fact that Nitrogen is considered a gas with constant concentration over time and has a Raman spectra easy to be separated from the Rayleigh one.

Writing the lidar equation for elastic backscatter and the corresponding equation for the Raman detection, and by taking the ratio of the two equation and applying the same procedure in the calibration range, both instrument functions (for each channel) and Raman cross sections vanish and the aerosol backscatter coefficient can be computed as:

$$\begin{aligned} \beta_a^L(R) &= -\beta_m^L(R) + \frac{RCS^L(R)}{RCS^L(R_C)} \cdot \frac{N_{N_2}(R)}{N_{N_2}(R_C)} \cdot [\beta_a^L(R_C) + \beta_m^L(R_C)] \cdot \\ &\cdot \exp\left\{ \int_{R_0}^{R_C} [\alpha_m^R(r) - \alpha_a^L(r) - \alpha_m^L(r)] \cdot dr - \int_{R_0}^R [\alpha_m^R(r) - \alpha_a^L(r) - \alpha_m^L(r)] \cdot dr \right\} \end{aligned} \quad (5)$$

The aerosol extinction coefficient can be computed directly from the Raman signal:

$$\alpha_a^L(R) = \frac{d}{dR} \left\{ \ln \left[\frac{N_{N_2}(R)}{RCS^R(R)} \right] \right\} - (\alpha_m^L(R) + \alpha_m^R(R)) \cdot \left(1 + \left(\frac{\lambda_L}{\lambda_R} \right)^k \right) \quad (6)$$

These results represent the level 1 products for the characterization of aerosols. The level 2 products can be immediately calculated from them: lidar ratio, Angstrom exponents and color ratios (in case of multiwavelength detection).

Using simultaneously two wavelengths, Angstrom exponents can be computed based on the extinction or backscatter coefficients derived from lidar, as follows:

$$a_{\alpha} = \frac{\ln\left(\frac{\alpha_1}{\alpha_2}\right)}{\ln\left(\frac{\lambda_2}{\lambda_1}\right)} \quad \text{and} \quad a_{\beta} = \frac{\ln\left(\frac{\beta_1}{\beta_2}\right)}{\ln\left(\frac{\lambda_2}{\lambda_1}\right)} \quad (7)$$

The Angstrom coefficients are good indicators of particle size a_{α} and number concentration b_{α} but do not provide precise information on the aerosol size distribution or the shape of the particles [9]. The diffuser shape may be identified measuring the *depolarization* of the initial plane polarized laser light. The depolarization ratio may be used to distinguish between spherical (e.g. water droplets, with low depolarization ratios) or nonspherical (e.g. ice crystals, with high depolarization ratios) particles.

The depolarization ratio $\delta_a(R)$ is calculated as the ratio of cross (c) to parallel (p) polarization states of the backscatter radiation relative to the initial linear polarization plan of the emitted laser light [9]:

$$\delta_a(R) = C_s(R) \frac{S_c(R)}{S_p(R)} \tag{8}$$

where C_s is a calibration function taking into account the whole system depolarization effects and the differential detection on the two channels at 532 nm.

Aerosol optical depth (AOD) or aerosol optical thickness (AOT) is a quantitative measure of the extinction of solar radiation by aerosol scattering and absorption between the point of observation and the top of the atmosphere. It is a measure of the integrated columnar aerosol load and the single most important parameter for evaluating direct radiative forcing. AOD is calculated as the extinction coefficient integrated on an atmospheric path generally scaled at the zenith direction (indicating the range by Z instead of R):

$$AOD = \int_{Z_0}^Z \alpha_a(z) dz \tag{9}$$

Aerosol optical depths typically decrease with increasing wavelength and are much smaller for longwave radiation than for shortwave radiation. Values vary widely depending on atmospheric conditions, but are typically in the range 0.02–0.2 for visible radiation.

Because AOD is essentially an integral of the extinction coefficient - which in case of elastic lidars is estimated based on a proper value of the lidar ratio -it is very sensitive to small calibration errors and to a minor degree to the errors introduced by the method chosen to model the other components.

All the parameters described above have large errors attached. Therefore, only the combination of all can reduce

the uncertainty. Fig. below presents the distribution of those parameters for various aerosol classes, normalized to the highest value [12].

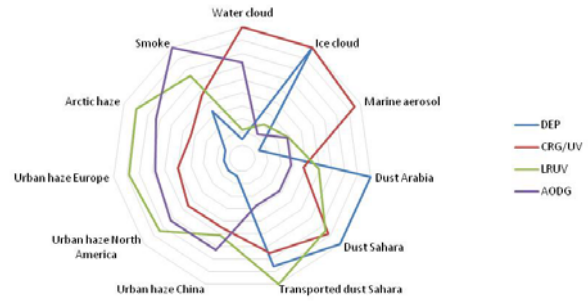


Fig. 2. Distribution of optical parameters for various aerosol classes, normalized to the highest value.

It is obvious that aerosol class can be assessed at the intersection of each sector in the diagram. First step is the identification of layers to be tested. A method to automatically compute layer's base and top is described in [14]. For each layer, average optical parameters are then calculated and compared to typical values for different aerosol classes.

3. Results and discussion

We present in the following 2 different cases for which further backtrajectories analysis was performed as confirmation for the algorithm outputs.

In Fig. 3 a Saharan dust event is shown. Backscatter coefficient profiles shows layers centered at 1.7 and 3.5 Km, while depolarization coefficient profiles shows different values for the 2 layers. The layer at 3.5 Km is depolarizing more than the one at 1.7 Km and significantly more than the PBL.

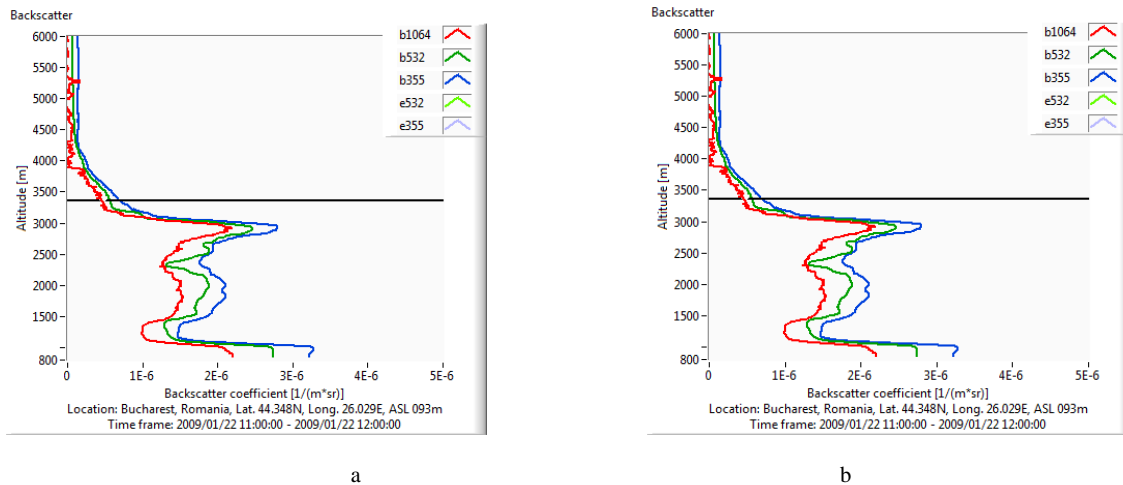


Fig. 3. Jan. 22, 2009: Saharan dust layer ~ 3Km: a) backscatter coefficient profiles at 1064, 532 and 355nm; b) depolarization ratio at 532 nm.

To confirm the results, HYSPLIT model was used to trace aerosol backward to the origin. Fig. 4 shows air masses at 1.5 Km coming from E Africa, while air masses at 3.5 Km are coming from Sahara. This confirms the output of our algorithm, which pointed out the 2 layers of being different in composition.

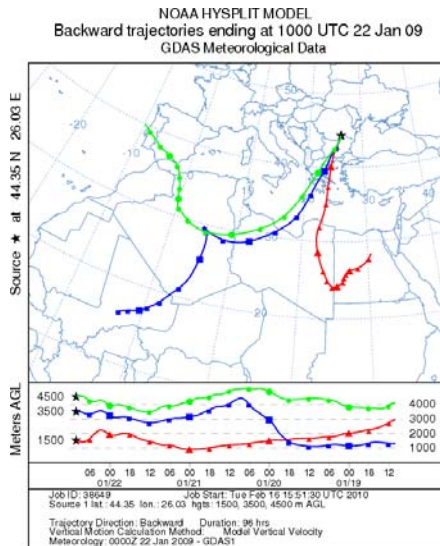


Fig. 4. Jan. 22, 2009: HYSPLIT backtrajectories for 1.5, 3.5 and 4.5Km.

DREAM model (Fig. 5) also predicted an important outbreak of the Saharan dust over Europe, and in Romania.

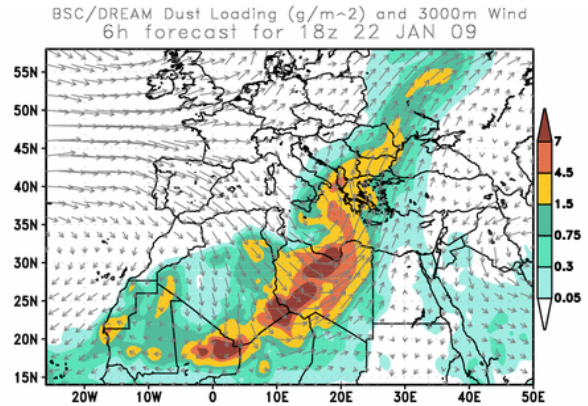


Fig. 5. Jan. 22, 2009: DREAM forecast.

In Fig. 6 a smoke episode is presented. In this case, aerosol layers are distributed up to 6 Km altitude (see backscatter coefficient profiles), but depolarization is quite low, almost the same as in the PBL.

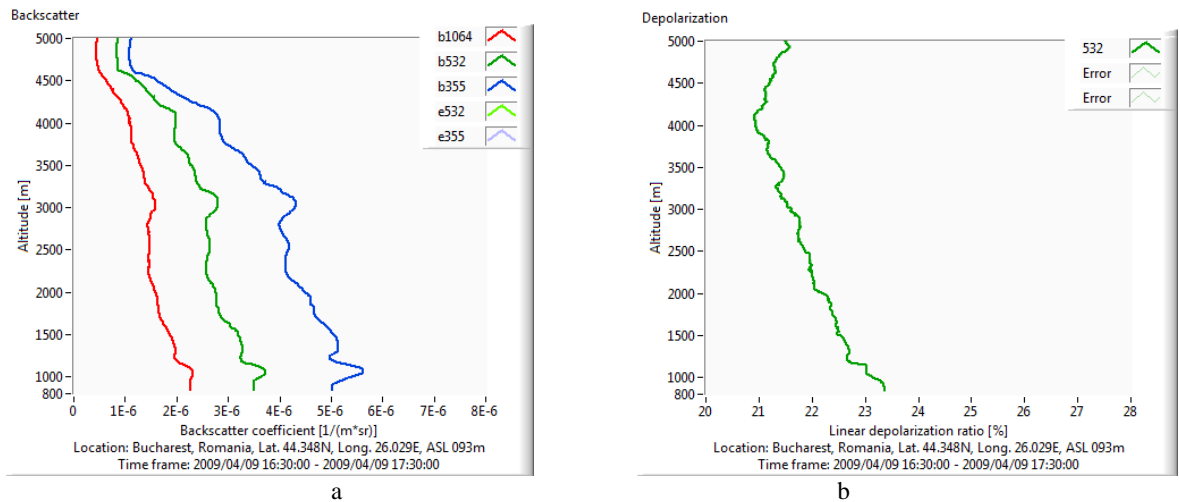


Fig. 6. Apr. 09, 2009: Smoke layers up to 7 Km: a) backscatter coefficient profiles at 1064, 532 and 355 nm; b) depolarization ratio at 532 nm.

Fig. 7 shows air masses at all 3 selected altitudes (2.0, 3.0 and 5.0 Km) coming from approx. the same region and travelling over Ukraine and Moldavia.

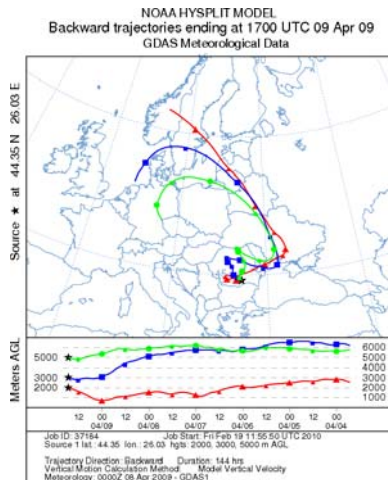


Fig. 7. Apr. 09, 2009: HYSPLIT backtrajectories for 2.0, 3.0 and 5.0 km.

For this case, MODIS fire map proved a high density of fires in those regions, which confirms again the results obtained from lidar.

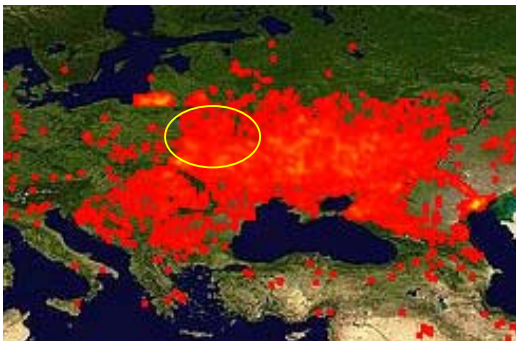


Fig. 8. Apr. 09, 2009: MODIS fire distribution.

4. Conclusions

The combination of lidar observations with in situ measurements and models provides a unique opportunity to conduct long-term inter-calibrations and complementary or simultaneous monitoring of different atmospheric parameters over various space-time scales.

During the past decade sophisticated computational procedures have been developed and successfully tested and can be used for the retrieval of microphysical properties of particles such as volume and surface-area concentration, effective radius, refractive index characteristics, and single-scattering albedo from optical data provided by lidars

Although quantitative data are always useful, errors associated to microphysical retrievals from lidar signals are usually so high that only the qualitative information can be used.

Using Lidar ratio, Angstrom coefficients and polarization ratios we depicted various types of aerosols (even mixed cases). We presented 2 cases of long-range transported plumes (aged mineral dust and smoke) detected by the multiwavelength Raman lidar in Bucharest, and confirmed by air mass trajectories analysis and satellite imagery.

Acknowledgements

This work was supported by grant no. STVES 115266 from Norway through the Norwegian Cooperation Programme for Economic Growth and Sustainable Development in Romania, and by grant no. 229907 through FP7-REGPOT-2008-1.

References

- [1] N. Braslau, J. V. Dave, *J. Appl. Meteorol.*, **12**, 616 (1973).
- [2] A. Hodzic, B. Bessagnet, R. Vautard, *Atmos Environ*, **40**, 4158 (2006).
- [3] R. F. Zobel, Q. J. Roy. *Meteor. Soc.*, **92**, 196, (1966).
- [4] T. J. Method, T. N. Carlson, *Atmos Environ*, **16**, 53 (1982).
- [5] J. Haywood, P. Francis, O. Dubovik, M. Glew, B. Holben, *J. Geophys. Res.*, **108** (D13), 8471 (2003).
- [6] O. Dubovik, M. D. King, *J. Geophys Res*, **105**, 20, 673, (2000).
- [7] A. Papayannis, *Int J Remote Sens*, **16**, 3595 (1995).
- [8] D. Müller, U. Wandinger, A. Ansmann, *Appl Optics*, **38**, 2346 (1999a).
- [9] D. Müller, U. Wandinger, A. Ansmann, *Appl Optics*, **38**, 2358 (1999b).
- [10] C. Böckmann, I. Mironova, D. Müller, Schneidenbach L., Nessler R., *JOSA A*, **22**(3) 518 (2005).
- [11] I. Veselovskii, A. Kolgotin, V. Griaznov, D. Müller, U. Wandinger, D. Whiteman, *Appl Opt.*, **41**, 3685 (2002).
- [12] A. Nemuc, D. Nicolae, C. Talianu, E. Carstea, C. Radu, *Rom. Rep. Phys.*, **61**(2), 313 (2009).
- [13] J. Ackermann, *J. Atmos. Ocean. Tech.*, **15**, 1043 (1997).
- [14] C. Talianu, D. Nicolae, J. Ciuciu, M. Ciobanu, V. Babin, *J. Optoelectron. Adv. Mater.*, **8**(1), 243 (2006).

*Corresponding author: nnicol@inoe.inoe.ro